Available online at www.sciencedirect.com

ScienceDirect

journal homepage: www.keaipublishing.com/en/journals/geog;
http://www.jgg09.com/jweb_ddcl_en/EN/volumn/home.shtml

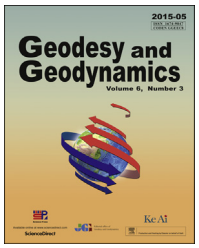

Deformation-strain field in Sichuan and its surrounding areas based on GPS data

Chen Fuchao[a,b,*], *Ta La*[b], *Chen Juzhong*[b]

[a] *School of Geodesy and Geomatics, Wuhan University, Wuhan 430079, China*
[b] *First Crust Monitoring and Application Center, China Earthquake Administration, Tianjin 300180, China*

ARTICLE INFO

Article history:
Received 21 October 2014
Accepted 17 January 2015
Available online 11 May 2015

Keywords:
Sichuan and its surrounding areas
Displacement vector field
Strain rate field
Fault activity
Strain–stress state in fault zone
Seismic belt
Deformation-strain field
Global Positioning System (GPS)

ABSTRACT

The strain rate in Sichuan and its surrounding areas, and the activity rate and strain rate in two block boundary fault zones were calculated according to the block movement parameters estimated using the station speed obtained from regional GPS station observation data in these areas for 2009–2011 and GPS continuous station data for 2011–2013. The movement field characteristics in these areas were analyzed with the Sichuan Basin as the reference. Results show that the principal strain rate and maximum shear strain rate of the Bayan Har block were the largest, followed by those of the Sichuan–Yunnan block and Sichuan Basin. The deep normal strain rate in the Longmenshan fault zone was compressive and large over the study period. The normal strain rate in the Xianshuihe fault zone was tensile.

1. Introduction

This study was performed for the region in the middle section of the North-South Seismic Belt that stretches across two major tectonic provinces, i.e., the eastern and western provinces, in China. The western province is located in Sichuan and contains the Bayan Har and Sichuan–Yunnan blocks of the Qinghai–Tibet subplate, which was affected by the structural development of the Himalayas, and the eastern province contains the Sichuan Basin of the South China subplate, which was affected by Pacific structural development. The May 12, 2008 Ms8.0 Wenchuan earthquake caused the seismically quiet Longmenshan fault zone to become seismically active, leading it to become an important area for geological studies [1–4]. Previous researchers analyzed the variation in the difference between the crustal movement field and strain field primarily based on the spatially continuous variations in the GPS rate [5–7]. A spatially continuous deformation field mainly reflects the shallow variations in the local crust and is relatively deficient in revealing the overall characteristics of deformation at depth and the strain–stress field of moving crustal blocks.

* *Corresponding author*. First Crust Monitoring and Application Center, China Earthquake Administration, Tianjin 300180, China.
E-mail address: chenfuchao1985@163.com (Chen F.).
Peer review under responsibility of Institute of Seismology, China Earthquake Administration.

Production and Hosting by Elsevier on behalf of KeAi

http://dx.doi.org/10.1016/j.geog.2015.04.001

Some studies have used block movement models to analyze block movement characteristics [8].

The Ms7.1 Yushu earthquake (April 14, 2010) and Ms7.0 Lushan earthquake (April 20, 2013) occurred in succession in Wenchuan and its surrounding areas several years after the Ms8.0 Wenchuan earthquake; therefore, it is necessary to conduct relatively in-depth studies on the recent activity related to the structure of Sichuan and its surrounding areas. The characteristics of the crustal deformation strain–stress field in the Sichuan region after the Ms8.0 Wenchuan earthquake served as the basis for studying the gestation and occurrence of the Lushan earthquake; repeated GPS measurements by the GPS network in China mainland since 2009 have laid the foundation for studying the current structural deformation in this region [9]. In this study, the block movement and strain parameters in Sichuan and its surrounding areas were calculated by block via a block movement model using GPS data for 2009–2011. The activity and strain–stress state of the shallow and deep parts of the main fault zones, i.e., the Longmenshan fault zone and the Xianshuihe fault zone, in this region were studied using regional network data for 2009–2011 and continuous observation station data for 2011–2013.

2. Calculation of stress–strain field

Based on observation data from the regional GPS network for 2009–2011 and the continuous stations for 2011–2013, we calculated the station rates under a global framework using the GAMIT/GLOBK software, and then grouped the GPS stations based on the geological tectonic units. Then, we calculated the movement field and strain field of various tectonic blocks, the strain–stress state in the block boundary fault zone caused by block movement and interaction, and the block activity using the block movement equation (1) [10]. For details on the division of structural areas and fault zones in the calculation, please refer to references [5–8,10–13].

$$\begin{bmatrix} v_e \\ v_n \end{bmatrix} = r\begin{bmatrix} -\sin\phi\cos\lambda & -\sin\phi\sin\lambda & \cos\phi \\ \sin\lambda & -\cos\lambda & 0 \end{bmatrix}\begin{bmatrix} \omega_x \\ \omega_y \\ \omega_z \end{bmatrix} + \begin{bmatrix} A_0 & B_0 \\ B_0 & C_0 \end{bmatrix} \times \begin{bmatrix} x \\ y \end{bmatrix} + \frac{1}{2}\begin{bmatrix} \xi_1 & \xi_2 \\ \zeta_1 & \zeta_2 \end{bmatrix}\begin{bmatrix} x^2 \\ y^2 \end{bmatrix} + \begin{bmatrix} \xi_3 \\ \zeta_3 \end{bmatrix} xy \tag{1}$$

where, ω_x, ω_y, and ω_z are rotation parameters, and A_0, B_0, C_0, ξ_1, ξ_2, ξ_3, ζ_1, ζ_2, and ζ_3 are strain parameters. The left side of the equation is the station rate, where V_e is the east-west movement component, and V_n is the south-north movement component. The first term on the right side of the equation is the overall rotation movement, and the second, third, and fourth represent continuous deformations in a block.

3. Movement field

Fig. 1 shows the movement vectors of the Bayan Har block and the Sichuan–Yunnan rhombus block relative to the Sichuan Basin calculated based on GPS observations in 2009 and 2011. As shown in the figure, the western part of the Bayan Har block in the study region is moving in the NEE direction, and the eastern part is moving SSE. The movement rate of the western part is relatively large, at 18.77 mm/a, and that of the eastern part is 8.77 mm/a; the difference is 10 mm/a, and the movement rate decreases gradually from west to east, reflecting compression in the eastern part.

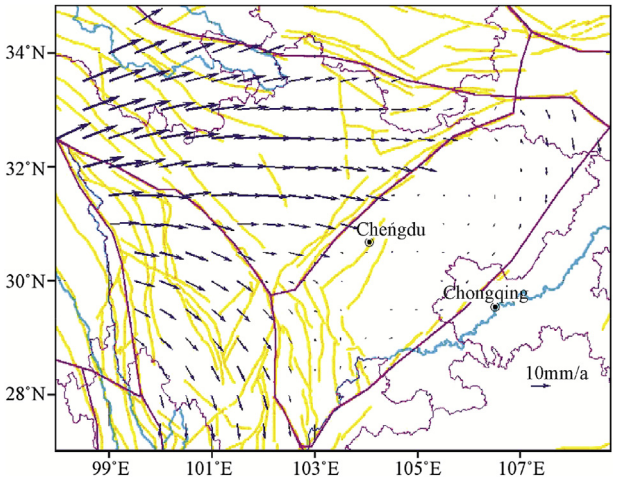

Fig. 1 – Horizontal movement field in Sichuan and its surrounding areas during 2009–2011.

The displacement vectors of the Sichuan–Yunnan rhombus block show that the northern and southern parts are moving eastwards and southwards, respectively, and the movement direction turns gradually from north to south. The movement rate of the northern part is 18.31 mm/a, and that of the central part is 8.15 mm/a; the difference is more than 10 mm/a. The directions of the displacement rate vectors of the Sichuan–Yunnan rhombus block change rapidly from E→SE→S from north to south, and the block mainly exhibits a clockwise rotation movement around the western part.

The movement difference in the Sichuan Basin is relatively weak; the northern part is moving southwards at a rate of 4.42 mm/a, while the southern part is moving insignificantly, indicating that the Sichuan Basin is relatively stable.

4. Principal strain field

The GPS station rates during 2009–2011 were grouped by block unit and the strain rates were calculated; the results are shown in Fig. 2. In the Bayan Har block, the average principal compressive strain rate is -24.59×10^{-9}/a, the principal compressive strain axis direction is NE88.7°, the principal tensile strain rate is 25.37×10^{-9}/a, and the principal tensile strain axis direction is NW358.7°. In the central and western parts of the Bayan Har block in the study region, the principal compressive strain rate, principal compressive strain axis direction, and principal tensile strain rate are -32.49×10^{-9}/a, NE68.1°, and 32.81×10^{-9}/a, respectively, in the northern area; -14.81×10^{-9}/a, SE94.0°, and 14.29×10^{-9}/a, respectively, in the central area; and -20.37×10^{-9}/a, SE129.9°, and 22.24×10^{-9}/a, respectively, in the southern

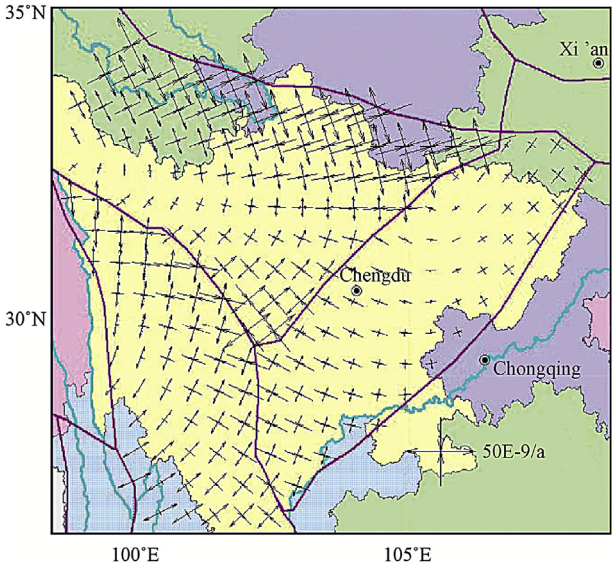

Fig. 2 – Horizontal strain field in Sichuan and its surrounding areas during 2009–2011.

area. The principal compressive strain rate is largest in the northern area, followed by the southern area, and it is relatively small in the central area; the principal compressive strain rate shows evident differences in different sections. Near the Longmenshan fault zone in the eastern part of the Bayan Har block in the study region, the principal compressive strain rate, the principal compressive strain axis direction, and the principal tensile strain rate are -31.63×10^{-9}/a, SE105.3°, and 27.74×10^{-9}/a, respectively. From north to south in the Bayan Har block in the study region, the principal compressive strain axis direction turns gradually NEE → EW → SEE; the principal tensile strain rate is slightly larger than the principal compressive strain rate in the central and western parts, and opposite in the eastern part.

In the Sichuan–Yunnan rhombus block, the average principal compressive strain rate, principal compressive strain axis direction, and principal tensile strain rate are -14.92×10^{-9}/a, SE130.1°, and 20.67×10^{-9}/a, respectively. The principal compressive strain rate and the principal compressive strain axis direction are -19.59×10^{-9}/a and SE97.7°, respectively, in the northern part of the block; and -12.09×10^{-9}/a, and SE127.9°, respectively, in the central part. The principal compressive strain axis turns gradually SEE → SE from north to south, and the principal compressive strain rate decreases somewhat.

In the Sichuan Basin, the average principal compressive strain axis direction, average principal compressive strain rate, and principal tensile strain rate are NE67.5°, -12.24×10^{-9}/a, and 6.48×10^{-9}/a, respectively. The principal compressive strain axis direction and principal compressive strain rate are NE64.0° and -10.82×10^{-9}/a, respectively, in the northern part of the basin, and SE103.5°, and -15.68×10^{-9}/a, respectively, in the southern part. The principal compressive strain axis direction turns NEE → SEE from north to south, and the principal compressive strain rate in the north is smaller than that in the south.

The above shows that the principal compressive strain axis varied regularly, turning from NEE to SE on the whole in the Bayan Har block, the Sichuan–Yunnan block, and the Sichuan Basin. The principal compressive strain rate is relatively larger in the northern and southern parts of the Bayan Har block and relatively small in the center; relatively larger in the northern part of the Sichuan–Yunnan block and relatively small in the middle; and relatively larger in the southern part of the Sichuan Basin and relatively small in the northern part. Among the three blocks, the Bayan Har block has the largest principal compressive strain rate, followed by the Sichuan–Yunnan block and the Sichuan Basin.

5. Maximum shear strain rate

The maximum shear strain rates in Sichuan and its surrounding areas calculated from block parameters are shown in Fig. 3. The maximum shear strain rate is over 100×10^{-9}/a, occurring in the Bayan Har block in the northwest of the study region. The minimum shear strain rate is below 10×10^{-9}/a, occurring in the middle of the Sichuan Basin. The maximum shear strain rate in the Bayan Har block increases from 20×10^{-9}/a to over 100×10^{-9}/a from south to north. The maximum shear strain rate in the Sichuan–Yunnan block decreases gradually from 50×10^{-9}/a to 20×10^{-9}/a from northeast to southwest. The shear strain rates in the Sichuan Basin are within $10–40 \times 10^{-9}$/a, being small in the center and slightly large in the south and north.

The Longmenshan fault zone, as a block boundary, has relatively dense isolines of maximum shear strain rate; the maximum shear strain rate differs significantly on both sides of the fault zone; in particular, the maximum shear strain rate decreases from 80×10^{-9}/a on the western side of the northeast section of the fault zone to 10×10^{-9}/a on the eastern side. There is a difference of 30×10^{-9}/a in the maximum shear strain rate between the eastern and western sides of the southwest section. The Xianshuihe fault zone mainly exhibits a turning belt of isolines of the maximum shear strain rate and

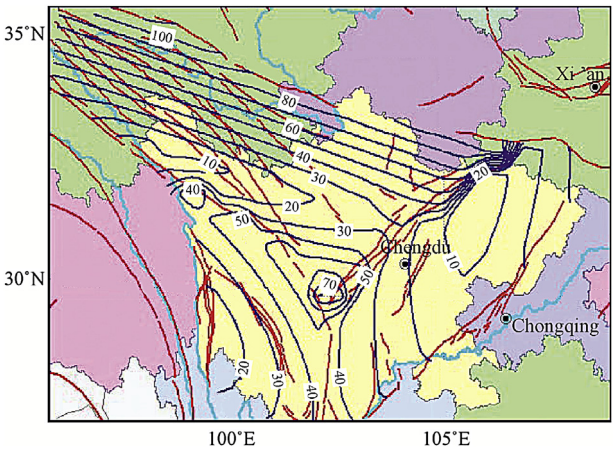

Fig. 3 – Maximum shear strain rate in Sichuan and its surrounding areas during 2009–2011 (isoline unit: 1×10^{-9}/a).

the differences in the rate are not as intense as those in the Longmenshan fault zone.

6. Activities in the fault zone

Activity at a boundary fault between active blocks is controlled by the non-uniform activity between the two adjacent blocks. The activity in a boundary fault zone depends on the different movement states of the adjacent blocks under different action forces. Therefore, the activity at a boundary fault reflects the overall activity of the adjacent blocks; in other words, the overall activity of the blocks can represent the activity at the boundary fault. It is well known that the overall block activity is a result of deep tectonic movements, and therefore, in this study, the activity rate and strain rate in the boundary fault calculated from the overall activity parameters of the blocks are considered to represent the activity at depth in the boundary fault zone, and the activity rate and strain rate in the fault calculated from the station rates near the boundary fault are considered to represent the state of the shallow crustal activity in the fault. Therefore, the deformation strain characteristics and stress states at the two boundary fault zones, i.e., the Longmenshan fault zone and the Xianshuihe fault zone, were analyzed for both the shallow and deep areas. These two fault zones are also important active earthquake zones in Sichuan and its surrounding areas.

6.1. *The Longmenshan fault zone*

(1) Deep activity

The strain rate perpendicular to the strike of a fault zone is defined as the normal strain rate along the strike of the fault zone, and it determines the compressive or tensile activity state of the fault. The shear strain rate parallel to the strike of a fault zone (i.e., the shear strain rate in a fault zone) determines the strike slip activity in the fault. The Longmenshan fault zone is the boundary zone between two Class I active blocks, i.e., the South China block, and the Qinghai–Tibet block, and therefore, the parameters of the South China block and Qinghai–Tibet block were calculated with equation (1). Then, the rates of the corresponding points on both sides of the fault zone were solved with the obtained parameters, and the activity rate in the fault zone was obtained by subtracting the rates of the corresponding points. The results are shown in Fig. 4. The fault dislocation vectors in the figure show the movement of the South China block wall relative to the Qinghai–Tibet block wall. The dislocation vector direction and dislocation rate were NW280.3° and 12.93 mm/a, respectively during 2009–2011. The overall strike of the Longmenshan fault zone was NE45° and the fault dislocation vectors intersected obliquely with the strike of the fault zone; the displacement vectors show that the fault is dominated by squeezing, and also has dextral strike slip movement, with a strike slip component of −7.25 mm/a and a squeezing component of −10.63 mm/a. During 2011–2013, the dislocation rate and the dislocation direction were 11.87 mm/a and NW296.63°, respectively, with a strike slip component of −3.79 mm/a and compression rate of −11.25 mm/a. The fault zone dislocation rates indicate that the fault movements during 2011–2013 were still dominated by squeezing.

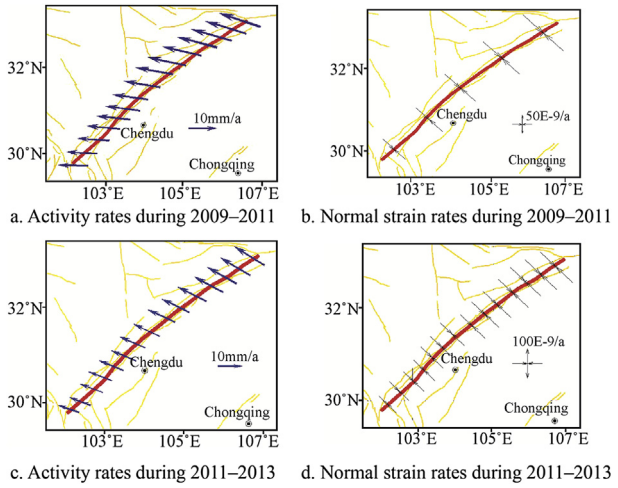

Fig. 4 – Deep activity in the Longmenshan fault zone.

During 2009–2011, the maximum and minimum normal strain rates in the Longmenshan fault zone were -80.60×10^{-9}/a and -142.48×10^{-9}/a, respectively, with an average of -110.61×10^{-9}/a. The normal strain rate was negative, indicating compression. The shear strain rate in the Longmenshan fault zone was -62.05×10^{-9}/a on average, with a maximum of -25.51×10^{-9}/a and minimum of -83.29×10^{-9}/a, exhibiting dextral shear.

During 2011–2013, the normal strain rate in the Longmenshan fault zone was -116.63×10^{-9}/a on average, with a maximum and minimum of -83.78×10^{-9}/a and -146.31×10^{-9}/a, respectively, indicating squeezing. The shear strain rate in the Longmenshan fault zone was -28.27×10^{-9}/a on average, with a maximum of -53.53×10^{-9}/a, indicating that dextral shear was dominant.

During the two time periods, i.e., 2009–2011, and 2011–2013, both the dislocation rate and normal strain rate in the Longmenshan fault zone indicate that squeezing activity was dominant, with the minimum normal strain rate reaching below -1×10^{-7}/a and the strain energy being accumulated rapidly.

(2) Shallow activity

The strain displacement rate vector and normal strain rate in the fault were calculated with the parameters obtained from the GPS station movement rates near the fault zone, and they reflect the strain–stress state and activity state at the shallow layer of the fault in the upper crust. The dislocation rate in the Longmenshan fault zone was calculated for the southeast wall relative to the northwest wall with the northwest wall of the fault zone as the reference. During 2009–2011, the shallow strain displacement rate vectors in the Longmenshan fault zone pointed to the fault, indicating significant compressive activity. The included angle between the vector direction and fault strike decreased and the vector direction and fault strike exhibited oblique intersection, with increase

in the strike slip movement in the southwest section compared to the northeast section of the fault. The dislocation rate in the fault was 2.99 mm/a on average, with a dextral strike slip rate of −1.43 mm/a and compression rate of −2.57 mm/a (Fig. 5a).

During 2009–2011, the shallow normal strain rate in the Longmenshan fault zone was -24.30×10^{-9}/a on average, with a maximum and minimum of -14.53×10^{-9}/a and -29.16×10^{-9}/a, respectively, exhibiting compressive activity (Fig. 5b). The shallow shear strain rate in the Longmenshan Fault was -29.78×10^{-9}/a on average, exhibiting dextral shear.

During 2011–2013, the shallow dislocation rate and dislocation direction in the Longmenshan fault zone were 1.16 mm/a and SW255.3°, respectively, with a dextral strike slip rate component of −1.00 mm/a and compression rate component of −0.59 mm/a (Fig. 5c). The shallow activity rate in the Longmenshan fault zone indicates that the fault was dominated by dextral strike slip during this time.

During 2011–2013, the shallow normal strain rate and shear strain rate in the Longmenshan fault zone were -5.00×10^{-9}/a and -18.47×10^{-9}/a, respectively (Fig. 5d). On the whole, the strain rates were small, and the shear strain rates were larger than the normal strain rates, exhibiting squeezing-dextral shear.

In summary, the activity at depth in the Longmenshan fault zone during 2009–2011 and 2011–2013 were dominated by squeezing, with normal strain rates being relatively large and compressive and shear strain rates being relatively small. The shallow activity was evidently smaller than that at depth. The shallow normal strain rate and shear strain rate differed little during 2009–2011, and the shear activity was stronger than the squeezing activity during 2011–2013.

6.2. *The Xianshuihe fault zone*

(1) Deep activity

Fig. 6 shows the activity rates and normal strain rates in the zone (Xianshuihe fault zone) between the Sichuan–Yunnan rhombus block and the Bayan Har block. The rate vectors in Fig. 6a express the change of the Bayan Har block relative to

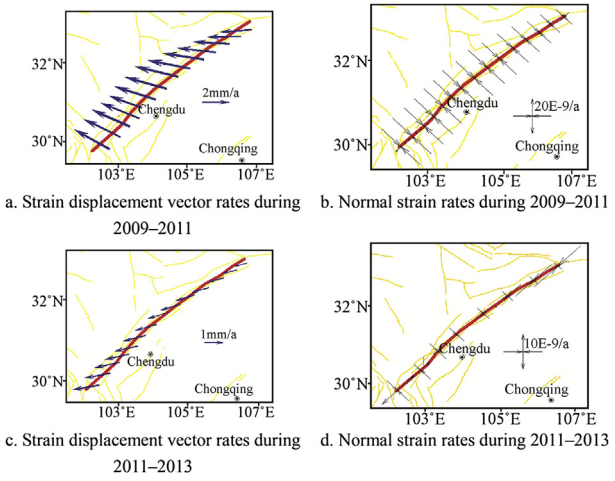

a. Strain displacement vector rates during 2009–2011
b. Normal strain rates during 2009–2011
c. Strain displacement vector rates during 2011–2013
d. Normal strain rates during 2011–2013

Fig. 5 – Shallow activity in the Longmenshan fault zone.

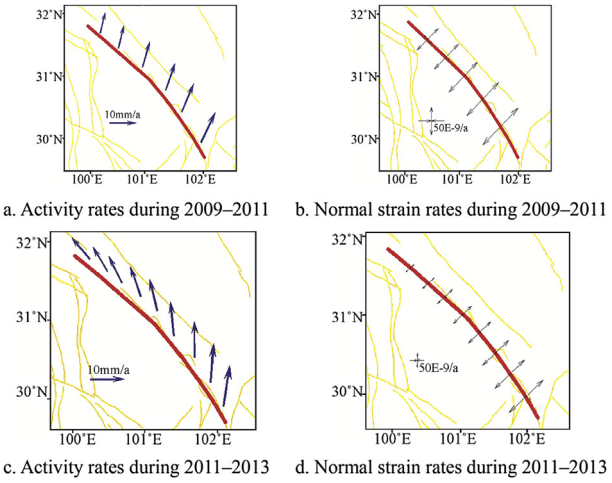

a. Activity rates during 2009–2011
b. Normal strain rates during 2009–2011
c. Activity rates during 2011–2013
d. Normal strain rates during 2011–2013

Fig. 6 – Deep activity in the Xianshuihe fault zone.

the Sichuan–Yunnan rhombus block. The Xianshuihe fault zone initially had a strike of NW during 2009–2011, the displacement vector direction intersected obliquely with the strike of the fault, with a relatively large included angle, and the fault was dominated by tensile activity and exhibited sinistral strike slip, with an average dislocation rate of 9.04 mm/a. The strike slip rate component and tensile rate component in the fault zone were 4.41 mm/a and 7.83 mm/a, respectively. During 2009–2011, the normal strain rate in the Xianshuihe fault zone was 74.55×10^{-9}/a on average, with a maximum and minimum of 94.65×10^{-9}/a and 55.21×10^{-9}/a, respectively. The normal strain rate was larger than 0, indicating tensile conditions (Fig. 6b). The shear strain rate in the Xianshuihe Fault was 46.66×10^{-9}/a on average, with a maximum and minimum of 66.04×10^{-9}/a and 25.83×10^{-9}/a, respectively. The shear strain rate was larger than 0, indicating sinistral activity.

During 2011–2013, the deep dislocation rate and dislocation direction in the Xianshuihe fault zone were 10.33 mm/a and NW349.6°, respectively, with a strike slip component of 7.89 mm/a, tensile component of 6.06 mm/a, and strike slip rate being slightly larger than the tensile rate. The normal strain rate in the Xianshuihe fault zone was 96.97×10^{-9}/a on average, with a maximum and minimum of 160.33×10^{-9}/a and 36.88×10^{-9}/a, respectively. The normal strain rate was larger than 0, indicating tensile conditions. The shear strain rate in the Xianshuihe fault zone was 130.17×10^{-9}/a, indicating sinistral shear.

In both time periods, the activity at depth in the Xianshuihe fault zone exhibited strike slip-tension, and the dislocation rate and strain rate in the latter time period were larger than those in the former. The strike slip (shear) activity in the latter time period was somewhat enhanced compared to that in the former.

(2) Shallow activity

During 2009–2011, the shallow strain displacement vector direction in the Xianshuihe fault zone was NW348.7°, deviating from the fault (Fig. 7a), and the fault exhibited tensile-

strike slip activity. The average activity rate, average strike slip component, and tensile component in the Xianshuihe fault zone were 2.69 mm/a, 2.10 mm/a, and 1.62 mm/a, respectively; the strike slip component was larger than the tensile component.

During 2009–2011, the normal strain rate in the Xianshuihe Fault was 24.97 × 10^{-9}/a on average, with a maximum and minimum of 50.52 × 10^{-9}/a and 4.35 × 10^{-9}/a, respectively. The normal strain rate was larger than 0, indicating tensile activity (Fig. 7b). The shear strain rate in the Xianshuihe fault zone was 67.70 × 10^{-9}/a on average, with a maximum and minimum of 85.63 × 10^{-9}/a and 56.36 × 10^{-9}/a, respectively. The shear strain rate was positive, indicating sinistral shear.

During 2011–2013, the displacement vector intersected obliquely with the strike of the fault zone (Fig. 7c), the average dislocation direction in the fault was NW327.8°, deviating from the fault. The activity rate was 0.48 mm/a on average, being relatively large in the southeast section and relatively small in the northwest section. The normal strain rate in the Xianshuihe fault zone was 7.02 × 10^{-9}/a on average (Fig. 7d), with a maximum and minimum of 10.30 × 10^{-9}/a and 4.18 × 10^{-9}/a, respectively. The normal strain rate was positive, indicating tensile activity. The shear strain rate in the Xianshuihe fault zone was 29.60 × 10^{-9}/a. The shear strain rate is evidently larger than the normal strain rate, reflecting that shear activity was relatively strong during this time period.

In summary, during both 2009–2011 and 2011–2013, the shallow shear activity in the Xianshuihe fault zone was relatively strong, and the tensile activity was relatively weak; the fault zone exhibited tensile and torsional activity on the whole.

6.3. *Activity and major earthquake gestation in the fault zones*

There are differences in the activity at depth between the Longmenshan fault zone and the Xianshuihe fault zone in both time periods. At depth, the Longmenshan fault zone was dominated by compression, and also included dextral shear, while the Xianshuihe fault zone exhibited tensile sinistral shear.

The normal strain rate at depth in the Longmenshan fault zone reached above −1 × 10^{-7}/a during both 2009–2011 and 2011–2013, and that in the latter time period was larger than that in the former time period; the high squeezing strain rate enabled the rapid accumulation of strain in the fault zone and the gestation and occurrence of strong earthquakes. The rapid accumulation of strain in the Longmenshan fault zone during the two time periods was a necessary precondition for the gestation and occurrence of the Ms7.0 Lushan earthquake on April 20, 2013. The normal strain rate at depth in the Xianshuihe fault zone was smaller than that in the Longmenshan fault zone, with tensile activity occurring during both time periods on the whole. The tensile action in the fault zone was favorable neither for locking nor for the accumulation of strain energy.

The shear strain rates at depth in the Longmenshan fault zone during 2009–2011 and 2011–2013 were −(25.51–83.29) × 10^{-9}/a and −(28.27–53.53) × 10^{-9}/a, respectively, exhibiting dextral shear; those in the Xianshuihe fault zone during 2009–2011 and 2011–2013 were (66.04–25.83) × 10^{-9}/a and 130.17 × 10^{-9}/a, respectively, exhibiting sinistral shear. On the whole, the shear strain rates in the Xianshuihe fault zone were larger than those in the Longmenshan fault zone. The large shear strain rates in the fault zones were helpful for strike slip movement and dislocation in the fault.

Strong compressive normal strain in a fault zone is favorable for fault locking and accumulation of strain energy, and is an important condition for the gestation and formation of strong earthquakes. There was also strong squeezing activity in the northwest of the Yushu fault zone before the Ms7 Yushu earthquake [14].

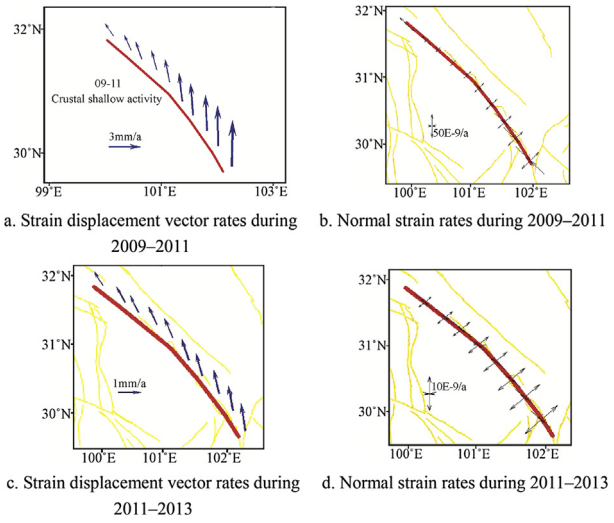

a. Strain displacement vector rates during 2009–2011

b. Normal strain rates during 2009–2011

c. Strain displacement vector rates during 2011–2013

d. Normal strain rates during 2011–2013

Fig. 7 – Shallow activity in the Xianshuihe fault zone.

7. Conclusions

(1) The displacement rate vectors in the crust of the Sichuan region show that, in the study region, the Bayan Har block belonging to the Qinghai–Tibet subplate moved toward NEE–E, the Sichuan–Yunnan block moved toward E–SE–S, and both of them basically changed continuously. The displacement rate vector direction of the Sichuan–Yunnan block changed relatively rapidly. The Sichuan Basin belonging to the South China subplate had a very small displacement rate vector, indicating it was relatively stable.

(2) The principal compressive strain rates of various blocks in the Sichuan region reveal that, during 2009–2011, the Bayan Har block in the study region had a relatively large principal compressive strain rate, the Sichuan–Yunnan block had a moderate principal compressive strain rate, and the Sichuan Basin had the smallest principal compressive strain rate. The principal compressive strain axis distribution reflects that the principal compressive stress axis exhibited a NEE–EW strike in the Bayan Har block, SE strike in the

Sichuan–Yunnan block, and NEE–EW–SEE strike in the Sichuan Basin.

(3) The station shear strain rates in the Sichuan region show that the Bayan Har block had the largest shear strain rate, with the maximum reaching over 100×10^{-9}/a, followed by the Sichuan–Yunnan block, and the Sichuan Basin.

(4) The activity at depth in the Longmenshan fault zone during 2009–2011 and 2011–2013 was dominated by squeezing, with a relatively large and compressive normal strain rate and a relatively small shear strain rate. The shallow activity was evidently weaker than that at depth. The normal strain rate at depth and the shear strain rate differed little during 2009–2011, and the shear activity was stronger than the squeezing activity during 2011–2013.

(5) The activity rates at depth and the normal strain rates in the fault zones calculated from the block movement parameters reveal that different block movements caused the differences in the activity and strain–stress state in the boundary fault zones. Although the shallow activity in the fault zones helped in the gestation of strong earthquakes, they were not as intense as the activity at depth. Therefore, obtaining the dislocation rate and normal strain rate of a fault zone from block movement parameters can help in the evaluation and understanding of the strain energy accumulation degree and risk of major earthquakes in a fault zone. The shallow activity intensity was evidently lower than that at depth in the fault zones in the study area.

Acknowledgments

This research is supported financially by Project under Science for Earthquake Resilience, China Earthquake Administration (XH13037Y).

REFERENCES

[1] Zhang Peizhen, Xu Xiwei, Wen Xueze, Ran Yongkang. Slip rates and recurrence intervals of Longmenshan active fault zone and tectonic implications for mechanism of the May 12 Wenchuan earthquake. Chin J Geophys 2008;51(4):1066–73 [in Chinese].

[2] Xu Xiwei, Wen Xueze, Ye Jianqing, Ma Baoqi, Chen Jie, Zhou Rongjun, et al. The Ms8.0 Wenchuan earthquake surface ruptures and its seismogenic structure. Seismol Geology 2008;30(3):597–629 [in Chinese].

[3] Jiang Zaisen, Fang Ying, Wu Yanqiang, Wang Min, Du Fang, Ping Jianjun. The dynamic process of regional crustal movement and deformation before the Ms8.0 Wenchuan earthquake. Chin J Geophys 2009;52(2):505–18 [in Chinese].

[4] Teng Jiwen, Zhang Yongqian, Yan Yanfen. Deep process of the rupture of strong earthquakes and exploration for impending earthquake prediction. Chin J Geophys 2009;52(2):428–43 [in Chinese].

[5] Wang Qi. Current crustal movement in Chinese mainland. Acta Seismol Sin 2003;25(5):453–64 [in Chinese].

[6] Ding Kaihua, Li Zhicai, Zou Rong, Wang Qi. Model analysis of crust motion in the Chinese mainland by CMONOC. Geodesy Geodyn 2014;5(4):1–8 [in Chinese].

[7] Zhang Peizhen, Shen Zhengkang, Wang Min, Gan Weijun. Kinematics of present-day tectonic deformation of the Tibetan plateau and its vicinities. Seismol Geology 2004;26(3):367–77 [in Chinese].

[8] Jiang Zaisen, Ma Zongjin, Zhang Xi, Wang Qi, Wang Shuangxu. Horizontal strain field and tectonic deformation of China mainland revealed by preliminary GPS result. Chin J Geophys 2003;46(3):352–8 [in Chinese].

[9] Li Yanxing, Zhang Jinghua, Zhou Wei, Hu Xinkang, Guo Liangqian, Zhang Zhongfu. The mechanism and dynamics of the generation and occurrence for the Ms8.0 Wenchuan earthquake. Chin J Geophys 2003;46(3):519–30 [in Chinese].

[10] Li Yanxing, Zhang Jinghua, He Jiankun, Li Jinling, Li Zhi, Guo Liangqian, et al. Current-day tectonic motion and intraplate deformation-strain field obtained from space geodesy in the Pacific plate. Chin J Geophys 2007;50(2):437–47 [in Chinese].

[11] Dong Yunhong, Luo Sanming, Han Yueping, Chen Changyun. Co- and post-seismic vertical displacements of the Ms8.0 Wenchuan earthquake near Beichuan. J Geodesy Geodyn 2011;2(2):29–32 [in Chinese].

[12] Guo Liangqian, Bo Wanju, Yang Guohua, Chen Juzhong, Guo He. Recent crustal movement and great earthquakes in Qinghai-Tibet sub-plate. J Geodesy Geodyn 2011;2(3):50–5 [in Chinese].

[13] Zhu Yiqing, Liu Fang, Liang Weifeng, Xu Yunma. Gravity variation associated with Wenchuan earthquake in western Sichuan. J Geodesy Geodyn 2011;2(1):55–60 [in Chinese].

[14] Guo Liangqian, Bo Wanju, Yang Guohua, Hu Xinkang, Guo He, Chen Changyun. The variation of the deformation-strain field before the Ms7.1 Yushu earthquake. Chin J Geophys 2011;54(8):1990–6 [in Chinese].

Chen Fuchao, a Ph.D candidate in School of Geodesy and Geomatics, Wuhan University, majored in geodesy and geophysics. He is mainly engaged in the research on deformation measurement and solid earth geophysics. His interests focus on the stability of the benchmarks in leveling survey by using GPS rate and movement characteristics of fault zone.